AIAA 80-1372R

Measured Molecular Absorptivities for a Laser Thruster

M. C. Fowler*
United Technologies Research Center, East Hartford, Conn.

One mechanism for powering a rocket engine with laser energy is the absorption of the latter by a molecular seed in the low molecular weight working fluid, hydrogen. Of interest, therefore, is the knowledge of the temperature dependence of the coupling molecule's absorption coefficient at the laser wavelength while immersed in the working fluid. To obtain the information at 10.6 μm wavelength for H_2O, D_2O, and NH_3 in H_2, measurements were carried out using a Mach Zehnder interferometer with a CO_2 laser light source. Measurements at temperatures as high as 6000 K were obtained using a plasma, sustained in the mixture by a second focused high power cw CO_2 laser beam, as a heat source. In addition, measurements at temperatures close to 4000 K were obtained without the plasma simply by focusing the high power beam into the mixture. H_2O and D_2O exhibited absorptivities as high as 1 cm^{-1}, more than an order of magnitude larger than expected from prior analysis, and NH_3 proved to be surprisingly stable at high temperatures, thereby enhancing the potential of these three molecules as couplers for the laser powered rocket.

Nomenclature

$E(y)$	= experimentally observed property
$I_c(y)$	= measured probe beam intensity passing through cell with plasma present
$I_c^0(y)$	= measured probe beam intensity passing through cell; no plasma present
$I_i(y)$	= measured interferometer throughput with plasma present
$I_i^0(y)$	= measured interferometer throughput; no plasma present
$I_n(y)$	= measured emission from plasma
$I_r(y)$	= measured reference beam intensity with plasma present
$I_r^0(y)$	= measured reference beam intensity; no plasma present
K	= mixture absorption coefficient
k	= Boltzmann constant
$n(x,y)$	= mixture index of refraction with plasma present
$n^0(x,y)$	= mixture index of refraction; no plasma present
$\Delta P(y)$	= absorption of probe beam passing near plasma
p	= mixture pressure
r	= radial distance to plasma axis
r_0	= upper limit of r
T	= mixture temperature
u	= absorber concentration
x	= coordinate parallel to probe beam axis
x_0	= upper limit of x
y	= coordinate normal to x and plasma axis
α	= mixture polarizability
$\Delta\phi(y)$	= interferometer phase angle change due to plasma presence
ρ	= mixture density

I. Introduction

ONE possible application for high power lasers involves using a ground based laser to supply energy to a distant rocket for orbit changes and other maneuvers. The remotely-based power plant is attractive in that the source of energy does not have to be launched, and a low molecular-weight working fluid, such a hydrogen, may be used for high specific thrust. One way of coupling the incident laser energy to the working fluid involves absorption of the energy by a molecular seed in the working fluid followed by collisional deactivation of the excited seed with resultant heating of the fluid. Of primary interest to this application is knowledge of the absorption coefficient of the seed/H_2 mixture over the temperature range of interest, from ambient to about 6000 K.

The absorptive properties of H_2O, D_2O and NH_3 in H_2 at 10.6 μm wavelengths was recently analyzed by Fowler et al.[1] in a study which included the temperature dependence of the chemical[2,3] as well as the spectroscopic properties of H_2O,[4,5] D_2O,[6] and NH_3[7] immersed in H_2, previous measurements involving NH_3 and D_2O being confined to 300 K. The H_2O measurements were averaged over 25 cm^{-1} wide intervals and extended to 3000 K. The work described in Ref. 1 extrapolated these data to 6000 K in 10 atm H_2 and one atmosphere of absorber. For H_2O a maximum absorption of 0.1 cm^{-1} was calculated. D_2O exhibited a higher absorption at temperature below 1500 K, but hydrogen atom exchange with H_2 is expected to convert the D_2O to H_2O at higher temperatures so that 0.1 cm^{-1} was again calculated as the maximum absorption. Finally, NH_3 was calculated to be a strong, 0.7 cm^{-1} amagat^{-1}, absorber at 300 K with thermal decomposition destroying its effectiveness at higher temperatures. To test these analytical results, measurements were carried out to determine CO_2 laser line absorption per cm as a function of temperature for temperatures as high as 6000 K, and the results of these measurements are the subject of this paper.

To attain the pressure/temperature conditions desired, the mixture was placed in a pressure cell, and a plasma was first created in the mixture by laser induced gas breakdown and then sustained by the focused output of a second 7 kW cw CO_2 laser. The resulting plasma was free of electrode material, and, since the sustaining laser beam was cylindrically symmetric and since the heat loss channels of radial thermal diffusion and bouyancy driven convection were also symmetric about the laser axis which was parallel to the force of gravity, the plasma was symmetric about the laser axis.

For studying the properties in the heated regions near such symmetric heat sources, the technique of Abel inversion[8] is used as it was in past studies of the spatial distribution of electron temperature and number density in laser sustained plasmas such as the one used in this study.[9,10] If z is the axis of symmetry, then in any xy plane normal to z, the observed quantity E measured along the x direction at a distance y from the zx plane is given by

$$E(y) = 2\int_0^{(r_0^2-y^2)^{1/2}} \epsilon(r)\,dx \qquad (1)$$

Presented as Paper 80-1372 at the AIAA 13th Fluid and Plasma Dynamics Conference, Snowmass, Colo., July 14-16, 1980; submitted Sept. 18, 1980; revision received Feb. 19, 1981.

*Experimental Physicist, Experimental Optics.

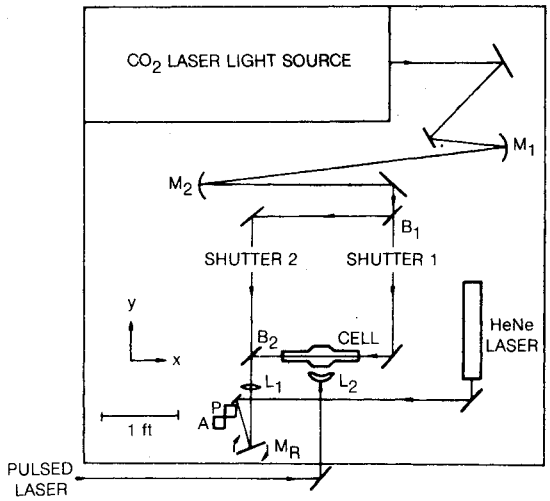

Fig. 1 Diagnostic apparatus. The pulsed laser is used to create plasma in the cell, and the cw laser, entering the cell normal to the plane of the figure, sustains the plasma.

where $\epsilon(r)$ vanishes for r greater than r_0. With $E(y)$ measured, $\epsilon(r)$ is obtained from the expression

$$\epsilon(r) = -\frac{1}{\pi}\int_r^{r_0} \frac{dE(y)}{dy}(y^2 - r^2)^{-1/2}dy \tag{2}$$

In principle, obtaining the temperature dependence of the absorption per cm, Ku, of the mixture involves performing such inversions on a simple transmission measurement and on some temperature diagnostic such as an interferogram and then correlating the two results. To yield accurate results, such a procedure needs a highly accurate aligning of the diagnostics spatially and temporally. The results presented in this paper were obtained using a diagnostic in which the transmission and temperature measurements are made simultaneously and coaxially, giving accurate Ku vs T curves free of errors arising from lack of spatial correlation.

II. Diagnostic Apparatus

The apparatus is shown schematically in Fig. 1. The cell containing the mixture to be studied was placed as shown in one arm of a Mach Zehnder interferometer upon a sliding stage to permit the center of the plasma formed within the cell to be moved horizontally along the y axis with respect to the interferometer light beam. The latter originated from a 9W CO_2 electric discharge laser operating on the P(18) transition. The beam from this laser passed through the telescope, made up of mirrors M_1 and M_2, to be expanded in size prior to entering the interferometer to a diameter of about 14 mm. Upon emerging from the interferometer at beamsplitter B_2, the CO_2 laser beam passed through lens L_1 and onto the rotating mirror M_R which swept the beam across the gold doped germanium detector A, equipped with a mask and an 0.2 mm pinhole, whose output was thus the y dependent intensity of the beam emerging at B_2. To ensure that in reducing the data the intensity readings to be compared refer to the same position on the y axis, the beam from the helium-neon (HeNe) laser was also directed onto M_R and thence to the pin diode detector whose output was superimposed on that from A, giving a data record consisting of a short, negative voltage spike corresponding to the HeNe beam followed by the broader positive voltage curve which was proportional to the CO_2 beam intensity. The mirror M_R rotated at 4000 rpm so that the time interval between successive data records was 15 ms.

Under conditions where absorption of energy from the high power laser beam, by either the plasma or simply the gas mixture alone, was high, density gradients within the cell were large enough to cause considerable refraction of the CO_2 probe laser light. Uncorrected, this refraction caused large errors in determining the y dependent absorption and phase angle shift, and the lens L_1 was placed as shown in Fig. 1 to reduce this problem. The germanium lens L_1 had a 20 cm focal length, and was positioned to image the axis of the high power laser within the cell onto the pinhole of detector A. As a result, all refraction effects occurring near the high power beam axis were removed as far as their effect on the measurement of the beam intensity profile at the detector A was concerned.[11]

In order to obtain both power loss and phase shift information, two shutters, herein referred to as shown on Fig. 1, were used. Shutter 1 was a Princeton Applied Research Model 125A operating in a manner so as to chop the beam going through the cell at a rate of 2000/min so that this beam was swept across detector A on every other revolution of the mirror. Shutter 1 was equipped with a light emitting diode and detector which operated to provide an output voltage whenever shutter 1 was open. This voltage was fed into a Tektronics FG504 function generator the output of which was used to trigger shutter 2, a Laser Precision CTX534 Radiation Chopper, in such a manner that the latter was locked on to chopping the beam through the reference side of the interferometer at half the rate that shutter 1 chopped the beam passing through the cell. As a result, on four successive rotations of M_R, detector A received the following information: first, with both shutters open, the interferometer throughput $I_i(y)$; second, the shutter 1 closed and shutter 2 open, the throughput of the reference side of the interferometer only, $I_r(y)$; third, with shutter 1 open and shutter 2 closed, the throughput of the cell only, $I_c(y)$; fourth, with both shutters closed no laser intensity was seen by the detector, but any detectable spontaneous emission occurring in the cell as a result of the presence of plasma was recorded by the detector, $I_n(y)$.

Assuming that no spontaneous emission was detected so that $I_n(y)$ was zero, the absorption $\Delta P(y)$ and phase angle change $\Delta\phi(y)$ were calculated from intensity profiles measured with plasma present combined with those obtained prior to the establishment of plasma, denoted by the superscript zero:

$$\Delta P(y) = \ln(I_r(y)/I_c(y)) + \ln(I_c^0(y)/I_r^0(y)) \tag{3}$$

$$\Delta\phi(y) = \cos^{-1}\left(\frac{I_i(y) - I_r(y) - I_c(y)}{2(I_r(y)I_c(y))^{1/2}}\right) - \cos^{-1}\left(\frac{I_i^0(y) - I_r^0(y) - I_c^0(y)}{2(I_r^0(y)I_c(y))^{1/2}}\right) \tag{4}$$

When spontaneous emission was detected, the quantities $I_i(y)$, $I_r(y)$ and $I_c(y)$ were corrected for this simply by subtracting $I_n(y)$ from each. It is thus seen that the quantities $\Delta P(y)$ and $\Delta\phi(y)$ were obtained from information collected in two 45 ms intervals, respectively, located after and prior to the establishment of the laser sustained plasma.

As can be seen from the foregoing discussion, complete data sets consisting of $I_i(y)$, $I_r(y)$, $I_c(y)$ and $I_n(y)$ were collected at the rate of about 17 s^{-1} for a total of nearly 100 sets for a 6 s long data collecting interval, and it was necessary to find a means of storing this mass of data until it was convenient to analyze it. This was done by storing the data signal on magnetic tape.

Each data record, consisting of the HeNe and CO_2 probe laser intensity profiles, was 200 μs long for the beam dimension, M_R rotation rate and M_R-to-A distances used in these experiments. From each data record, detailed and accurate intensity information had to be obtained for use in Eqs. (3) and (4). To do this, each selected 200 μs long voltage trace stored on the magnetic tape was digitized and stored as a 512 element array on an IBM Diskette 1 type "floppy disk."

III. Data Reduction

Prior to their use in Eqs. (3) and (4), the data records, now consisting of 512 element numerical arrays, were finally adjusted to ensure first that the given address in each array referred to the same value of y by aligning the HeNe voltage spikes in each record and second, that the base line of each array was correctly zeroed.

As indicated by Eq. (4), obtaining $\Delta\phi$ involves values of ϕ obtained from data sets taken prior to and during the presence of the laser supported plasma. However, the only directly calculable values of ϕ lie between $-\pi$ and 0, and there is therefore a second array, $-\phi$, corresponding to the same values of $\cos\phi$. There is therefore the ambiguity as to which of the quantities, $\phi-\phi^0$, $\phi+\phi^0$, $-\phi-\phi^0$, $-\phi+\phi^0$ accurately describes $\Delta\phi$.

This ambiguity was resolved by considering the physical situation giving rise to $\Delta\phi$. The phase shift is given in terms of the change in the index of refraction, n, along the path $(-Px_0,x_0)$ traversed by the beam

$$\Delta\phi(y)=\frac{2\pi}{\lambda}\int_{-x_0}^{x_0}(n(x,y)-n^0(x,y))\,dx \tag{5}$$

where λ is the radiation wavelength, 10.6 μm. The index of refraction is related to the gas pressure, p, and temperature T as well as the polarizability of the gas α according to [12]

$$n=2\pi p\alpha/kT \tag{6}$$

It is seen that $\Delta\phi(y)$ is negative and since, as in the present experiments, the temperature distribution has cylindrical symmetry with a maximum on the axis, which is the high power laser beam axis, then $\Delta\phi(y)$ passes through a minimum at $y=0$. With this knowledge, $\Delta\phi$ is obtained first by examining the profiles of the four quantities described above and deciding which is most likely to describe $\Delta\phi$ based on its shape and the position of its minimum compared to the position of the plasma center as determined from the position of maximum detected plasma spontaneous radiation.

The task of fitting $\Delta P(y)$ and $\Delta\phi(y)$ to an even powered polynomial in y was accomplished by use of a computer program. The y origin was assigned to the address observed to occur at the plasma center as indicated by $I_n(y)$. In these experiments the change in y per array address change is 54 μm. It is thus seen that the 200 μm pinhole causes the recorded data to be an array, over nearly four array addresses.

The value of r_0 is the value of y for which the polynomial fit first crosses zero. In the case of $\Delta\phi$, the procedure as described thus far does not permit accurate determination of the magnitude of the minimum in $\Delta\phi$. That is, the minimum calculated may differ from the actual value by an increment equal to an integral factor of 2π. For experiments in which the high power laser beam was simply focused into the gas mixture with relatively small interaction with it, the temporal variation in I_i was slow enough to permit accurate estimation of $\Delta\phi$, and it was found that in these cases the magnitude of $\Delta\phi$ was such that r_0 was equal to or slightly less than the distance of the z axis to the cell wall, 1.6 cm. When the high power beam-mixture interaction was intense, as in the presence of plasma, the initial transient in I_i was too fast to follow from the recorded data and so increments of -2π were added to the value of the minimum in $\Delta\phi$ until the calculated value of r_0 fell close to 1.6 cm.

Obtaining $k(r)u(r)$ from $\Delta P(y)$ was carried out in a quite straightforward manner, but the method of obtaining $T(r)$ from $\Delta\phi(y)$ merits more discussion at this point. Combining Eqs. (5) and (6) and substituting the density for p/kT, inversion results in calculation not of the temperature itself but rather the product of the density and the species averaged polarizability $\bar{\alpha}$ of the medium at radius r:

$$\rho(r)\bar{\alpha}(r)=(\lambda/4\pi^2)\epsilon_\phi(r)+\rho^0\bar{\alpha}^0 \tag{7}$$

where $\epsilon_\phi(r)$ is the value of $\epsilon(r)$ with $E(y)$ being $\Delta\phi(y)$. Assuming the establishment of chemical equilibrium and using literature values of the zero frequency polarizability of H_2, H and O_2 (Ref. 12), O (Ref. 13), and H_2O (Ref. 14), the species averaged polarizability was calculated for 10 atm H_2 and compared to that for 10 atm H_2 and 0.5 H_2O. The latter was found to exceed the former by 8% due to the large H_2O polarizability, but this difference vanished at around 3000 K due to the dissociation of H_2O. Due to the small size of this difference, the polarizability of a mixture originally pure H_2 was used in the temperature calculation. The density ρ^0 in Eq. (7) was obtained from readings of cell pressure, p_0, and temperature, T_0. In practice, the cell pressure during the experimental run was found to differ from p_0 by as much as 15% due to the heat addition from the high power laser beam. Accordingly, this pressure was used in obtaining the temperature at r from $\rho(r)\bar{\alpha}(r)$ and a calculated plot of $\rho(T)\bar{\alpha}(T)$ vs T.

As a result of this inversion, both the temperature and the absorption per cm were found as functions of radial position relative to the high power laser beam axis, thereby revealing the dependence of the latter upon the former.

IV. Experimental Results

Refraction Effects

In an experiment in which a laser beam is used to obtain spatially detailed information near a hot dense plasma which gives rise to steep temperature and refractive index gradients, the question arises as to what extent the latter causes significant refraction of the diagnostic laser beam and thereby affect the quality of the data. As mentioned earlier, the 20 cm

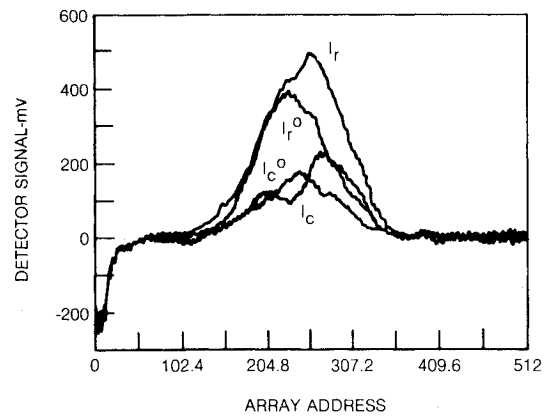

Fig. 2 Measured profiles I_r^0 and I_i^0 along with I_r and I_c in the presence of laser sustained plasma in 11 atm dry H_2.

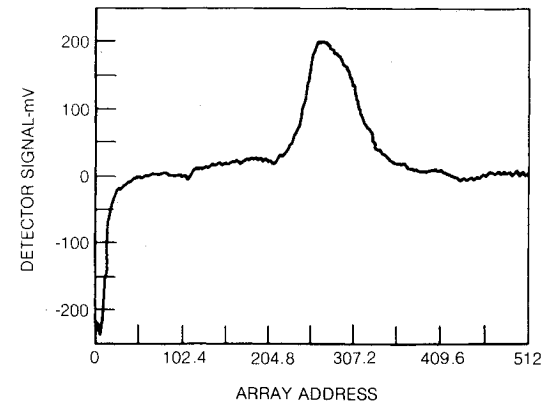

Fig. 3 Spontaneous emission profile I_n measured for the plasma of Fig. 2.

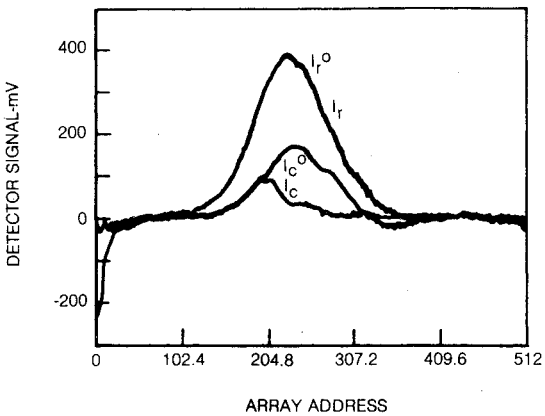

Fig. 4 Profiles I_r^o and I_i^o along with I_r and I_c after subtraction of I_n.

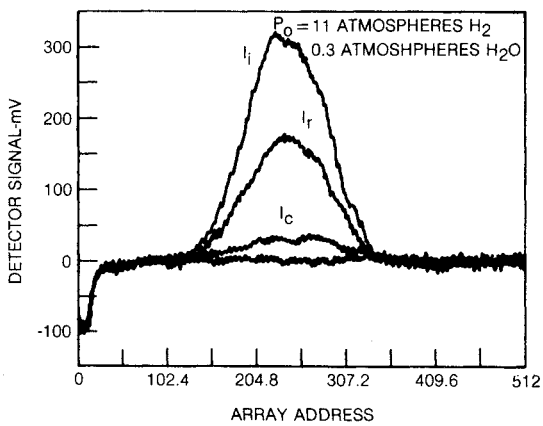

Fig. 5 Measured profiles I_i^o, I_r^o, and I_c^o before establishment of plasma.

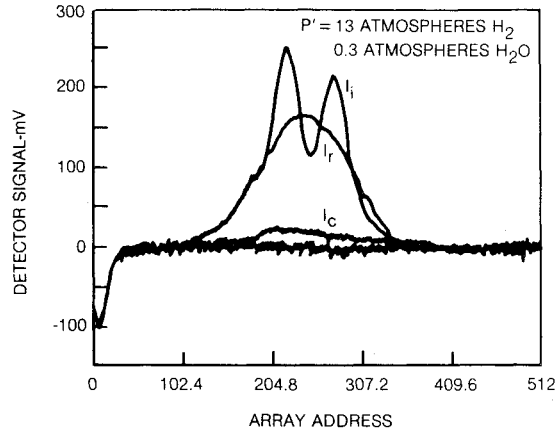

Fig. 6 Measured profiles I_i, I_r, and I_c after establishment of plasma.

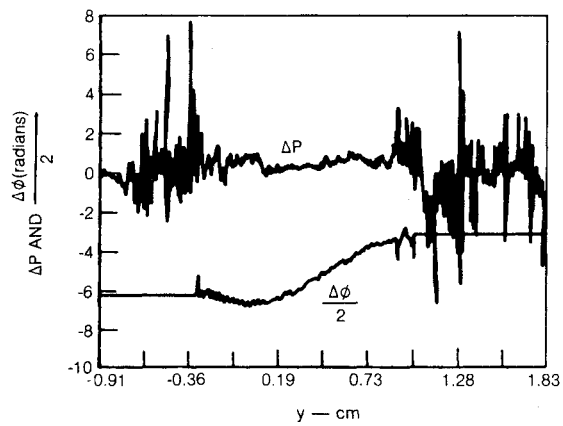

Fig. 7 Calculated arrays P and $\Delta\phi/2$ for the data shown in Figs. 5 and 6.

focal length lens was placed at the exit of the interferometer to correct such refraction effects, and this section describes the success obtained.

With the cell filled with H_2 at 150 psig, a laser sustained plasma was established and data taken as described in the previous sections. Figure 2 shows the arrays I_r, I_c, I_r^o, and I_c^o the former pair exhibiting substantial distortion due to spontaneous emission from the plasma, and Fig. 3 shows the array I_n containing the detected spontaneous emission. I_n was subtracted from I_r and I_c to eliminate the effect of the emission on the latter, and the same four arrays are replotted in Fig. 4. The attenuation of I_c by the plasma is seen to occur at nearly the same location as the onset of the radiation intensity. The exact separation between the two onsets is about 0.05 cm, with essentially no distortion in I_c occurring at points further away from this point which is 0.4 cm from the plasma core. When this data was fully reduced, the onset of absorption was calculated to occur at a radius of about 0.4 cm, where the temperature was calculated to be 8200 K, in substantial agreement with the results given for the onset of inverse bremstrahlung absorption in hydrogen in Ref. 15. Of more importance however, the fact that no distortion of I_r occurs at greater radial positions and lower temperatures, as expected for pure H_2, infers that refraction, even in the presence of plasma, has no significant effect on the data in the temperature region of interest to this study.

Example of Data Reduction

With the cell filled with hydrogen to a pressure of 11.0 atm, H_2 along with 0.3 atm H_2O, the recorded detector output appeared as shown in Fig. 5, and the presence of plasma in the cell had the effect shown in Fig. 6. Although the detected spontaneous emission in this experiment was not large enough to permit determination of the position of the high power laser beam axis, this property can be obtained from the calculated values of ΔP and $\Delta\phi$ which are shown as functions of the coordinate y in Fig. 7.

The data of Fig. 7 were inverted to give the radius dependent values and temperature which are shown in Fig. 8. In this experiment the probe beam intercepted the hot plasma core as well as the cooler region of interest to this study. The measured value of Ku therefore exhibits maxima at the axis, due to inverse bremstrahlung absorption, and at 0.7 cm from the axis due to H_2O absorption. As shown in the figure, the temperature regime in which H_2O is an active absorber extends from 1800 to 5800 K.

The inversion in each case was repeated with small variations in ΔP and $\Delta\phi$ as well as the cell temperature and pressure prior to the run and the observed cell pressure during the experiment. This was done to determine the sensitivity of the results to these quantities as well as to estimate the results' accuracy. It was estimated that the random uncertainty in the ΔP data was ± 0.1, and this variation resulted in the indicated uncertainty of ± 0.05 cm^{-1} on the axis and ± 0.15 cm^{-1} in the cooler region. In determining the temperature, it was found that the results exhibited the greatest sensitivity to the measured cell pressure, which, for the type of gage used, was $\pm 3\%$. This would result in a systematic, rather than random, error of $\pm 12\%$ near 2000 K and $\pm 36\%$ near 6000 K, and the corresponding error bars are shown in the figure.

Experimental Results

H_2O in H_2

The measured temperature dependence of Ku for H_2O in H_2 is shown in Fig. 9. The indicated H_2O partial pressure corresponds to the H_2O vapor pressure in a reservoir through

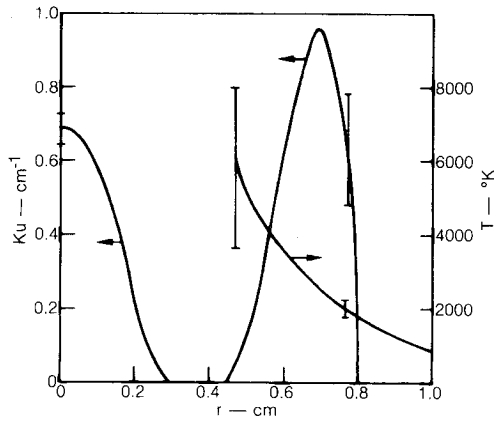

Fig. 8 Values of $Ku(r)$ and $T(r)$ obtained from the data in Fig. 7. The error bars are discussed in the text.

which the hydrogen was flowed prior to entering the cell. Also shown in the figure is the value of Ku for one atmosphere H_2O in 10 atm of H_2 as calculated in Ref. 1 based on the results of Ref. 5. The experimental curve corresponding to the results shown in Fig. 8 is marked with an asterisk.

The curve labeled "Flame data" deserves special attention. This result was obtained not in the presence of the laser sustained plasma but rather when the interaction between the focused high power laser beam and the gas mixture was intense enough to give rise to an orange, tenuously glowing volume in the focal region. It is seen that the temperature obtained in the center of the flame, 3000 K is comparable to that obtained in the cooler regions in the plasma experiments and that the Ku values in the two types of experiments agree essentially within the error limits indicated in Fig. 8.

The experimental results are not, however, in agreement with the analytically derived values of Ref. 1, having a maximum value of 1 cm^{-1}, at least a factor of five larger even though the H_2O concentration is a factor of three smaller. The reason for this difference is not known. One possible explanation is radiative excitation of the H_2O molecule causing its vibrational population distribution to be highly excited, thereby making possible absorption of probe beam energy by high lying H_2O energy levels. In the experiments involving the H_2O flame, excitation would result from the 10.6 μm radiation flux (in excess of a MW/cm^2) from the high power CO_2 laser. In addition, recent calculations given in Ref. 16 suggest that in the plasma experiments, the radiative flux from the plasma over all wavelengths could approach 0.1 MW/cm^2. Although smaller in magnitude than the CO_2 laser flux mentioned above, the wavelength distribution of the plasma radiation might include wavelengths which couple more effectively to H_2O, thus compensating for the lower total flux level.

D_2O in H_2

The experimental results for D_2O are shown in Fig. 10, which includes one curve obtained using a plasma heat source and two curves obtained from experiments in which a laser energized flame was obtained. In the latter cases, it is seen that, like H_2O, D_2O is capable of interacting with intense CO_2 laser radiation to produce high temperatures, as high as 4000 K in the curves shown. Also shown are two calculated results from Ref. 1. The curve labeled D_2O was calculated for the indicated H_2/D_2O mixture in which the only effect of increasing temperature was to lower the gas density and change the D_2O internal energy level population distribution. In practice, as the temperature increases the establishment of chemical equilibrium will cause D_2O to vanish, with H_2O and HDO becoming the dominant coupling molecules and these chemistry effects are included in the curve labeled H_2O. It is expected that at low temperatures the curve labeled D_2O would be valid with the H_2O curve becoming valid at higher

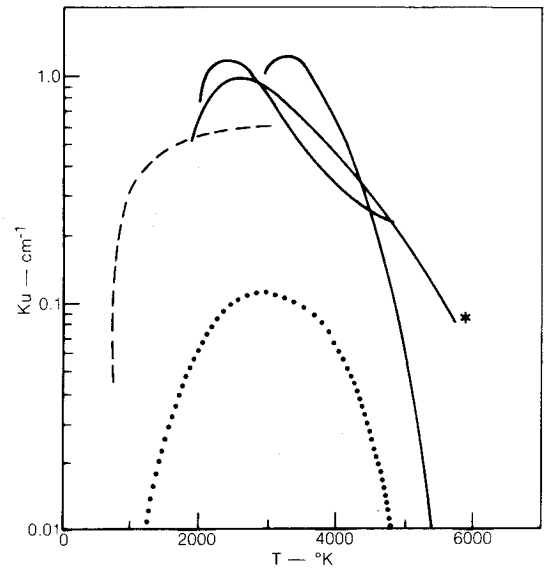

Fig. 9 $Ku(T)$ for 0.3 atm H_2O in 13 atm H_2: (—plasma data; ---flame data; · · · calculated for 1 atm H_2O in 10 atm H_2).

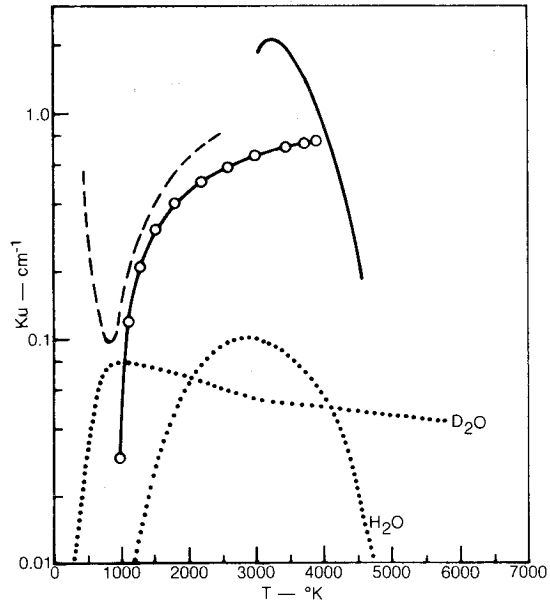

Fig. 10 $Ku(T)$ for D_2 in H_2: (—plasma data, 0.3 atm D_2O in 13 atm H_2; ---flame data 0.3 atm D_2O in 13 atm H_2; 0-0-0 flame data 0.1 atm D_2O in 11.4 atm H_2; · · · calculated 1 atm D_2O in 10 atm H_2).

temperatures when the rate of approach to chemical equilibrium is consistent with the time scale of the experiment. Examination of the dashed flame data curve indicates that in this experiment, the change-over from D_2O to HDO/H_2O as principle absorber occurs in the 500-900 K interval. More important, however, is the fact that like H_2O, D_2O exhibits a maximum Ku value of about 1 cm^{-1}, much larger than calculated analytically.

NH_3 in H_2

Like H_2O and D_2O, NH_3 formed a tenuous flame when irradiated with intense CO_2 laser radiation. In the presence of the plasma, the NH_3 concentration decreased markedly, presumedly due to thermal decomposition of the compound. In contrast, no such decomposition was detected in the flame experiments.

The $Ku(T)$ curve for the H_2/NH_3 system is shown in Fig. 11. The analytical study in Ref. 1 showed NH_3 to couple quite well to CO_2 laser radiation at room temperature but to

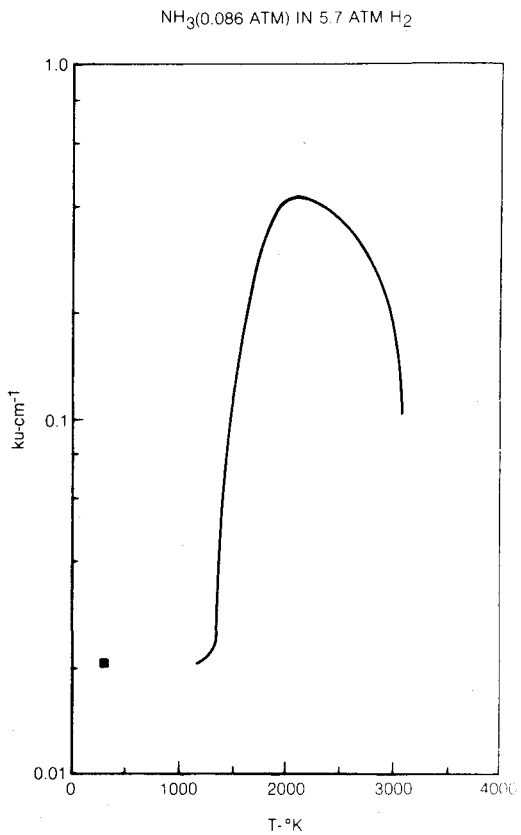

Fig. 11 $Ku(T)$ for a NH_3/H_2 mixture. The NH_3 pressure was obtained by chemical analysis. The square is the measured room temperature value.

decompose at temperatures above 500 K, thus apparently limiting its usefulness. The results in Fig. 11 are therefore surprising, for the value of *Ku* remains constant until 1000 K is reached, then increases more than an order of magnitude in value reaching a maximum near 2000 K. As was the case for the water molecules, energy level nonequilibrium caused by the intense radiation field may account for the large *Ku* values observed. The observed resistance to thermal decomposition in the flume experiments may be due to the slowness of the decomposition kinetics compared to the rate of diffusion of molecules through the high temperature zone.

Discussion of Results

The experimental results presented in this paper have significant implications for laser thruster performance. For the water molecules, the measured *Ku* values are significantly greater than expected from analysis using available data, as large as 1 cm^{-1} for the 0.3 atm partial pressures used, resulting in substantial reduction in the size and complexity of a laser thruster coupling chamber which could extract a significant fraction of the incident beam energy. In addition, all three molecules tested exhibited the ability, without preheating, to couple well to intense CO_2 laser radiation, the absorbing medium reaching temperatures in the 2000-4000 K laser thruster operating thrusting range, NH_3, in addition, not experiencing thermal decomposition in doing so. It would be of interest to determine whether such desirable properties are attainable for the laser power level and beam diameter and molecular concentrations expected to be used in a practical device, and the development of scaling laws for obtaining the laser energized molecular flame would therefore be desirable for the development of the laser thruster.

V. Summary

Using a novel diagnostic technique and heat source, the temperature dependent absorptivity was measured for H_2/H_2O, H_2/D_2O, and H_2/NH_3 at pressures between 5 and 10 atm and temperatures up to 6000 K. All three mixtures exhibited unexpectedly high (1 cm^{-1}) absorptivities compared to prior calculation and also the ability to obtain temperatures in the laser thruster operating range (2000-4000 K) by interacting, without preheating, with a 7 kW cw CO_2 laser beam. The mixtures studied therefore showed unexpected promise as coupling media for the laser energized rocket thruster.

Acknowledgment

This research was sponsored by the Air Force Rocket Propulsion Laboratory. The technical assistance of L. Muldrew, B. Doyle, J. Nycz, R. Basilica, and W. New is gratefully acknowledged.

References

[1] Fowler, M. C., Newman, L. A., and Smith, D. C., "Beamed Energy Coupling Studies," AFRPL-TR-79-51, 1979.

[2] Gordon, S. and McBride, B. J., "Computer Program for Calculation of Complex Chemical Equilibrium Compositions, Rocket Performance, Incident and Reflected Shock and Chapman-Jouget Detonations," NASA SP-273, 1971.

[3] Dixon Lewis, G., Sutton, M. M., and Williams, A., "The Kinetics of Hydrogen Atom Recombination," *Discussions of the Faraday Society*, Vol. 33, 1962, p. 205.

[4] McClatchey, R. A. et al., "AFCRL Atmospheric Absorption Line Parameters Compilation," AFCRL-TR-73-0096, 1973.

[5] Ludwig, C. B., "Measurements of the Curves of Growth of Hot Waver Vapor," *Applied Optics*, Vol. 10, 1971, p. 1057.

[6] Benedict, W. S., Gailor, N., and Plyler, E. K., "Rotation-Vibration Spectra of Deuterated Water Vapor," *Journal of Chemical Physics*, Vol. 24, 1965, p. 1139.

[7] Taylor, F. W., "Spectral Data for the ν_2 Bands of Ammonia with Applications to Radiative Transfer in the Atmosphere of Jupiter," *Journal of Quantitative Spectroscopy and Radiative Transfer*, Vol. 13, 1973, p. 1181.

[8] Griem, H. R., *Plasma Spectroscopy*, McGraw-Hill, New York, 1964, p. 176.

[9] Fowler, M. C. and Smith, D. C., "Ignition and Maintenance of Subsonic Plasma Waves in Atmospheric Pressure Air by cw CO_2 Laser Radiation and Their Effect on Laser Beam Propagation," *Journal of Applied Physics*, Vol. 46, 1975, p. 138.

[10] Keefer, D. R., Henriksen, B. B., and Braerman, W. F., "Experimental Study of a Stationary Laser-Sustained Air Plasma," *Journal of Applied Physics*, Vol. 46, 1975, p. 1080.

[11] Huddlestone, R. H. and Leonard, S. L., *Plasma Diagnostic Techniques*, p. 431 ff.

[12] Hirschfelder, J. O., Curtis, C. F., and Bird, R. B., *Molecular Theory of Gases and Liquids*, John Wiley and Sons, Inc., New York, 1954, pp. 340, 882.

[13] Nesbet, R. K., "Atomic Polarizabilities for Ground and Excited States of C, N, and O," *Physics Review A.*, Vol. 16, 1971, p. 1.

[14] Stillinger, F. H., *Theory and Molecular Models for Water in Non-Simple Liquids*, edited by I. Prigogine and S. A. Rice, John Wiley and Sons, New York, 1975, p. 1.

[15] Krascella, N. K., "Theoretical Investigation of the Spectral Optics of Hydrogen and Nuclear Fuel," AFSCR RTD-TDR-63-110, 1963.

[16] Park, C., "Calculation of Radiative Properties of Non-equilibrium Hydrogen Plasma," *Journal of Quantitative Spectroscopy and Radiative Transfer*, Vol. 22, 1979, p. 101.